

# Force Control based on Biarticular Muscle System and its Application to Novel Robot Arm Driven by Planetary Gear System

Sehoon Oh, Yasuto Kimura and Yoichi Hori

**Abstract**— We have suggested a novel statics and force control can be achieved in a more simple way by using the biarticular muscle coordinate. In order to verify these characteristics, a robot arm with two links that are driven by planetary gear is developed in this paper.

First, the complicated muscle structure is simplified as a three-pair six-muscle model including the biarticular muscle. Then based on the configuration, statics at the endeffector is redefined and a force control algorithm is suggested. The suggested statics and force control have the advantage of its simplicity.

Then a novel robot arm to emulate the biarticular muscle is developed. A planetary gear system is adopted to transfer torque generated by a motor to two joints. Unnecessary coupling caused by the planetary gear is removed by disturbance observer control. Experiments done by the robot arm verifies the effectiveness of the suggested statics and force control.

## I. INTRODUCTION

Analysis of the human muscle system and development of a robot manipulator that mimics human musculoskeletal system have been researched for several years. Some research focuses on the measurement of human impedance/stiffness characteristic [1],[2], others focus on the relationship between the stiffness and actual muscle [3].

However, there has been a big distance between these analyses of the human muscle system and its application to the control of robot manipulators [4],[5]. Especially, the biarticular muscle that has been said to play a significant role in human walking is not fully incorporated in robotics, since it is not analyzed from the view point of robotics. There has been some research on the role of biarticular muscle [6],[7], however the approach has been done in an inductive way based on experiments and biomechanical models. The complicated muscle characteristic has been hard to simplify and reflect in motor control.

In order to address this problem, we have developed an analysis methodology and control algorithm that connect these two systems[8]. Our work is intended to provide a deductive way of analyzing biarticular muscles by simplifying their force output characteristics in order to make the incorporation of the biarticular muscle in robotics easier.

In this paper, our suggestion is revisited and to show that statics and force control can be achieved in a more simple way by using the biarticular muscle coordinate. In order to verify these characteristics, a robot arm with two links that are driven by planetary gear is developed in this paper.

S. Oh and Y. Hori are with Department of Electrical Engineering, School of Engineering, University of Tokyo, 3-7-1 Hongo Bunkyo Tokyo, Japan  
sehoon@hori.k.u-tokyo.ac.jp

This paper is organized as follows; in Section II, three-pair six-muscle model is introduced as a simple model representing complicated muscle system. In Section III, novel statics is derived for a manipulator incorporating the biarticular muscle and verified by experiments. Finally, a novel robot arm that incorporate the biarticular muscle characteristic using a planetary gear system is developed in Section IV and the suggested force control is verified by the robot arm in Section V.

## II. APPLICATION OF BIARTICULAR MUSCLE TO ROBOTICS

### A. Introduction of Biarticular Muscle to Robot Arm

Real muscle configuration is complicated so we adopt the simplified 3-pair muscle structure describe in Figure 1: flexors and extensors of two monoarticular muscles and one biarticular muscle. Each flexor and extensor muscle generates the forces  $f_1^f$  to  $f_3^e$ . These forces can be simplified using the equivalence suggested in the last section.

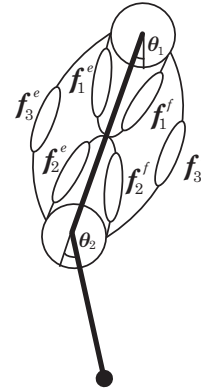


Fig. 1. Two-Joint Manipulator with Muscle Model

Equation (1) and (2) are the torques generated on two joints by 3 pairs of muscles.

$$\begin{aligned} T_1^j &= r_1(f_1^e - f_1^f) + r_1(f_3^e - f_3^f) \\ &= r_1(u_1^e - u_1^f) + r_1(u_3^e - u_3^f) - (u_1^e + u_1^f)K'_1r_1\theta_1 \\ &\quad - (u_3^e + u_3^f)K'_3r_1\theta_{12} \end{aligned} \quad (1)$$

$$\begin{aligned} T_2^j &= r_2(f_2^e - f_2^f) + r_2(f_3^e - f_3^f) \\ &= r_2(u_2^e - u_2^f) + r_2(u_3^e - u_3^f) - (u_2^e + u_2^f)K'_2r_2\theta_2 \\ &\quad - (u_3^e + u_3^f)K'_3r_2\theta_{12}, \end{aligned} \quad (2)$$

where  $r_i$  is the radius of the joint  $i$ ,  $K'_i$  means  $K_i + B_i s$  and  $\theta_{12}$  means  $\theta_1 + \theta_2$ . In Equations (1) and (2), the first two

terms are the difference mode which generates torques to rotate the joints, while the last two terms are the sum mode that is related to the stiffness around the joints.

Each extensor muscle force ( $f_i^e$ ) and flexor muscle force ( $f_i^f$ ) is defined as follows.

$$f^f = u^f + K u^f \Delta x + B u^f \Delta \dot{x} = u^f - u^f (K + B s) r \Delta \theta \quad (3)$$

$$f^e = u^e + K u^e \Delta x + B u^e \Delta \dot{x} = u^e + u^e (K + B s) r \Delta \theta, \quad (4)$$

where  $\Delta x$  is the contraction of muscle that can be describe as  $r \Delta \theta$

In this paper, three muscle torques generated by three pairs of muscles in Figure 1 are defined as the following, based on the muscle force equation (3),(4).

$$\tau_1^m = r(f_1^e - f_1^f) = r(u_1^e - u_1^f) - (u_1^e + u_1^f) K'_1 r \theta_1 \quad (5)$$

$$\tau_2^m = r(f_2^e - f_2^f) = r(u_2^e - u_2^f) - (u_2^e + u_2^f) K'_2 r \theta_2 \quad (6)$$

$$\tau_3^m = r(f_3^e - f_3^f) = r(u_3^e - u_3^f) - (u_3^e + u_3^f) K'_3 r (\theta_1 + \theta_2) \quad (7)$$

where  $r_1 = r_2 = r$  is assumed.

These muscle torque equations and Equation (1), (2) leads to the relationship between the joint torques  $T_1^j, T_2^j$  and the muscle torques  $\tau_1^m, \tau_2^m, \tau_3^m$  as the following.

$$\begin{pmatrix} T_1^j \\ T_2^j \end{pmatrix} = \begin{pmatrix} \tau_1^m + \tau_3^m \\ \tau_2^m + \tau_3^m \end{pmatrix} \quad (8)$$

Now, this analysis allows us to introduce a configuration of a novel manipulator illustrated in Figure 2, where the biarticular muscle is modeled as a linear motor producing the force  $F_m$ . This biarticular linear force  $F_m$  leads to the torque  $\tau_3^m$  in two joints at the same time.

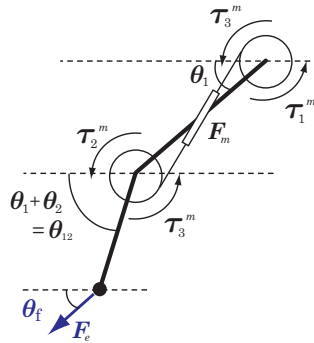


Fig. 2. Configuration of Two-link Manipulator with Biarticular Muscle

$\tau_1^m, \tau_2^m$  are the torques generated by monoarticular muscles of two joints, and  $\tau_3^m$  is the torque generated by a biarticular muscle tension  $F_m$ . The torques generated by these two monoarticular muscles and one biarticular muscle can be projected to the joint torques as Equation (8).

Note again that the torque by the biarticular muscle is added to two joints at the same time.

### III. NOVEL FORCE CONTROL BY BIARTICULAR MUSCLE

#### A. Simplification of Statics by Biarticular Muscle Configuration

Figure 3 is the configuration of a two-link manipulator.

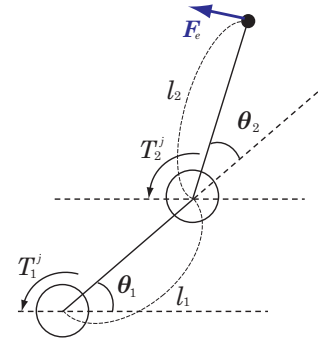


Fig. 3. Configuration of Two-link Manipulator

In the conventional manipulator configuration where two actuators are located in two joints, the balance between the forces applied on the endeffector and the joint torques also can be described using Equation (9), the Jacobian. Equation (10) is the relationship between the force  $F_e$  on the endeffector in Figure 3 and the joint torques ( $T_1^j, T_2^j$ ); the force  $F_e$  in Figure 3 is described as  $F_e = (f_x, f_y)^T$ .

$$J = \begin{pmatrix} -l_1 \sin \theta_1 - l_2 \sin(\theta_1 + \theta_2) & -l_2 \sin(\theta_1 + \theta_2) \\ l_1 \cos \theta_1 + l_2 \cos(\theta_1 + \theta_2) & l_2 \cos(\theta_1 + \theta_2) \end{pmatrix} \quad (9)$$

$$\begin{pmatrix} T_1^j \\ T_2^j \end{pmatrix} = J^T \begin{pmatrix} f_x \\ f_y \end{pmatrix} \quad (10)$$

The joint torques related to the endeffector force  $F_e$  is distributed to  $\tau_1^m, \tau_2^m, \tau_3^m$  in this section. In order to develop the relationship between the force on the endeffector and the muscle torques, the Jacobian needs to be modified. To this end, we use the relationship between  $\tau_3^m$  and the absolute angle  $\theta_{12}$ ; the absolute angle  $\theta_{12} = \theta_1 + \theta_2$  in Figure 2 can be defined as the output of the biarticular muscle. The point that  $\tau_3^m$  affects both joints supports this definition, and the dynamics of  $\tau_3^m$  derived in the following sections also shows this output definition is right.

Equation (10) can be divided into two parts like the following equation.

$$J^T \begin{pmatrix} f_x \\ f_y \end{pmatrix} = \begin{pmatrix} -l_1 \sin \theta_1 f_x + l_1 \cos \theta_1 f_y \\ 0 \end{pmatrix} + \begin{pmatrix} -l_2 \sin \theta_{12} f_x + l_2 \cos \theta_{12} f_y \\ -l_2 \sin \theta_{12} f_x + l_2 \cos \theta_{12} f_y \end{pmatrix} \quad (11)$$

Considering this, three muscle torques  $\tau_1^m, \tau_2^m, \tau_3^m$  which cope with the external force  $F_e$  can be defined as follows.

$$\tau_1^m = -l_1 \sin \theta_1 f_x + l_1 \cos \theta_1 f_y, \quad \tau_2^m = 0 \quad (12)$$

$$\tau_3^m = -l_2 \sin \theta_{12} f_x + l_2 \cos \theta_{12} f_y \quad (13)$$

The muscle torques  $\tau_1^m, \tau_2^m, \tau_3^m$  cannot be decided uniquely from the joint torques  $T_1^j, T_2^j$ . If, however, we ignore  $\tau_2^m$  intentionally, the relationship can be simplified and it will provide a new relationship between  $F_e$  and muscle torques as the following equation.

$$\begin{pmatrix} \tau_1^m \\ \tau_3^m \end{pmatrix} = \begin{pmatrix} -l_1 \sin \theta_1 & l_1 \cos \theta_1 \\ -l_2 \sin \theta_{12} & l_2 \cos \theta_{12} \end{pmatrix} \begin{pmatrix} f_x \\ f_y \end{pmatrix} = (J_{abs})^T \begin{pmatrix} f_x \\ f_y \end{pmatrix} \quad (14)$$

The absolute angle Jacobian matches well with the bi-articular muscle manipulator; using  $J^{abs}$ , the relationship between  $F_e$  and  $\tau_1^m, \tau_2^m, \tau_3^m$  can be written in a simple way as Equation (14).

### B. Novel Static Force Control based on Biarticular Muscle Force

When the magnitude and direction of  $F_e$  are given as  $F_e = (F \cos \theta_f, F \sin \theta_f)$ , the relationship with the muscle torque can be more simplified using  $J_{abs}$ .

$$\begin{pmatrix} \tau_1^m \\ \tau_3^m \end{pmatrix} = (J_{abs})^T \begin{pmatrix} F \cos \theta_f \\ F \sin \theta_f \end{pmatrix} = \begin{pmatrix} Fl_1 \sin(\theta_f - \theta_1) \\ Fl_2 \sin(\theta_f - \theta_{12}) \end{pmatrix} \quad (15)$$

Equation (15) is the proposed new kinematic equation which relates  $\tau_1^m, \tau_3^m$  to the characteristics of the external forces:  $F$  and  $\theta_f$ . With the biarticular muscle torque coordinate, the endeffector force can be designed in a more simple way; two muscle torques are just two functions of  $\theta_f, \theta_1, \theta_{12}$  and  $F$ .

In the following section, experiments are conducted to verify this relationship.

## IV. DEVELOPMENT BIARTICULAR MUSCLE IMPLEMENTED ROBOT ARM BASED ON PLANETARY GEAR SYSTEM

### A. Introduction of Planetary Gear System To Biarticular Muscle Implemented Robot Arm

Figure 4 shows the mechanism of the planetary gear system. The planetary gear system consists of a sun gear, planetary gears, a ring gear, and a planetary carrier. The sun gear is located at the center, and planetary gears revolve around the sun gear in rotation, and the ring gear surrounds these gears. The planetary carrier transmits a revolution of planetary gears.

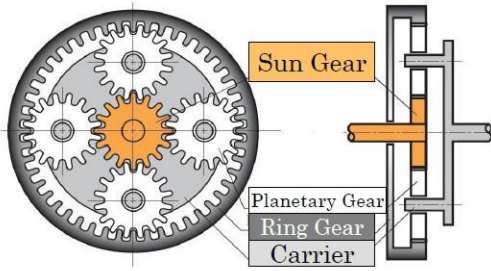


Fig. 4. Mechanism of planetary gear system

### B. Correspondence between gears and muscle torques

The relationship among these gears is somewhat complicated; there are four kinds of rotating gears connected with each other. This relationship in the planetary gear system does not match with the muscle system in Figure 1 or Figure 2. We need to rematch the gear torques with the muscle torques by some gear torque design strategy.

Figure 5 shows our strategy about the match of gears and motors. The motor which drives the ring gear works

as a mono-articular muscle rotating only the first joint or the shoulder. The motor which drives a sun gear works as a mono-articular muscle rotating only the second joint or the elbow. Lastly, the motor which drives a carrier works as the bi-articular muscle rotating both joints simultaneously.

In order to realize this correspondence, we need to design torques that will be applied to each gear. The methodology of this design will be given in Section IV-D. Before the design, we need to clarify the force relationship in the planetary gear system.

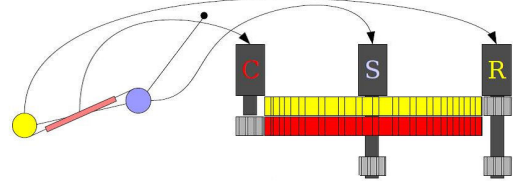


Fig. 5. Correspondence of gears to muscle torques

### C. Motion equation of planetary gear system

The motion equation of the planetary gear system can be derived based on Lagrangian mechanics. Table I is the nomenclature for this motion equation.

TABLE I  
PARAMETER OF PLANETARY GEAR SYSTEM

|            |                                      |
|------------|--------------------------------------|
| $\theta_r$ | rotation angle of ring gear          |
| $J_r$      | inertia of ring gear                 |
| $\tau_r$   | input torque of ring gear            |
| $\theta_s$ | rotation angle of sun gear           |
| $J_s$      | inertia of sun gear                  |
| $\tau_s$   | input torque of sun gear             |
| $\theta_c$ | rotation angle of carrier            |
| $\tau_c$   | input torque of carrier              |
| $J_c$      | inertia of carrier                   |
| $\theta_p$ | rotation angle of planetary gear     |
| $J_p$      | rotation inertia of planetary gear   |
| $\theta_o$ | revolution angle of planetary gear   |
| $J_o$      | revolution inertia of planetary gear |
| $\rho$     | gear ratio                           |

The planetary gear system is constrained by the following equations.

$$\theta_s - \frac{\rho - 1}{2\rho} \theta_p - \frac{\rho + 1}{2\rho} \theta_o = 0 \quad (16)$$

$$\theta_c = \theta_o \quad (17)$$

$$\theta_s + \frac{\rho - 1}{2} \theta_p - \frac{\rho + 1}{2} \theta_o = 0 \quad (18)$$

Lagrangian function is given as follows.

$$L = \frac{1}{2} J_r \dot{\theta}_r^2 + \frac{1}{2} J_s \dot{\theta}_s^2 + \frac{1}{2} J_p \dot{\theta}_p^2 + \frac{1}{2} J_o \dot{\theta}_o^2 - \tau_r \theta_r - \tau_s \theta_s - \tau_c \theta_c \quad (19)$$

Based on these constraints and Lagrangian function, torque transmissions to each joint can be derived as follows.

$$J_r \ddot{\theta}_r = K_1 \tau_r + K_2 \tau_s + K_3 \tau_c \quad (20)$$

$$J_s \ddot{\theta}_s = L_1 \tau_r + L_2 \tau_s + L_3 \tau_c \quad (21)$$

$K_1, K_2, K_3$  are torque transfer constants from each motor to the ring gear and  $L_1, L_2, L_3$  are torque transfer constants to the sun gear. If the inertial force of  $J_r \ddot{\theta}_r$  and  $J_s \ddot{\theta}_s$  are identified with the joint torques  $(T_1^j, T_2^j)$ , we can discover that there are some differences in these equations compared with Equation(8):

- There is unnecessary coupling; sun gear torque  $\tau_s$  and ring gear torque  $\tau_r$  that are supposed to work as mono-articular muscles affect other joints.
- Torque generated in the carrier gear affects two joint with a different ratio; torque transfer constant ( $L_3, K_3$ ) of the carrier gear torque are different with each other.

In order to resolve these problems, a planetary gear system needs some design methodology that will make the system work same with the muscle system.

#### D. Control of Planetary Gear Robot Arm

1) *Block diagram of a planetary gear system:* Figure 6 is a block diagram of the planetary gear system. This block diagram is based on Equation (20) and (21).  $K_2$  and  $L_1$  are influences from the other side mono-articular muscle and should be removed. Meanwhile,  $K_3$  and  $L_3$  are influences from the bi-articular muscle that should be identified with each other to generate the same torque in both joints.

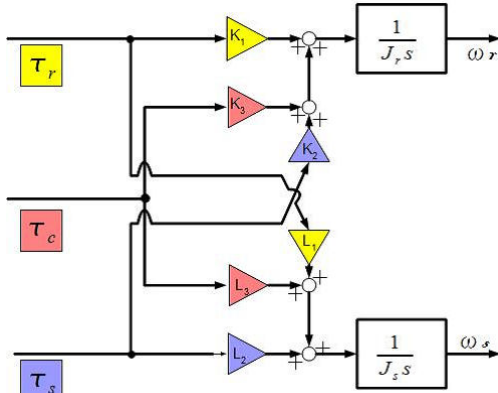


Fig. 6. Block diagram of a planetary gear system

2) *Feedforward design of carrier motor torque:* This design utilizes the carrier torque as a mean to separate the sun gear torque and ring gear torque in a feedforward way. Since the carrier can transmit its torque to both sides, it can negate the mutual interference between ring gear torque and sun gear torque. Design of the carrier torque is given as follows.

$$\tau_c^* = E_1 \tau_s + E_2 \tau_r + \tau_c^b, \quad (22)$$

where  $E_1$  is transfer constant of the sun gear to the ring gear and  $E_2$  is vice versa.  $\tau_c^b$  is the torque that will act as the

bi-articular muscle torque affecting both joints at the same time.

We will call these constants “isolation ratio”.  $\tau_c^*$  is the actual torque command that is given to the current controller of a motor that is connected to the carrier gear. With the appropriate design of the isolation ration  $E_1$  and  $E_2$ , the relationship of Equation (20) and (21) will be modified as follows.

$$\begin{aligned} J_r \ddot{\theta}_r &= (K_1 + K_3 \cdot E_1) \tau_r + (K_2 + K_3 \cdot E_2) \tau_s + K_3 \tau_c^b \\ &= (K_1 + K_3 \cdot E_1) \tau_r + K_3 \tau_c^b \end{aligned} \quad (23)$$

$$\begin{aligned} J_s \ddot{\theta}_s &= (L_1 + L_3 \cdot E_1) \tau_r + (L_2 + L_3 \cdot E_2) \tau_s + L_3 \tau_c^b \\ &= (L_2 + L_3 \cdot E_2) \tau_s + L_3 \tau_c^b \end{aligned} \quad (24)$$

The optimal design of  $E_1$  and  $E_2$  can be derived from this relationship as follows.

$$E_1 = -\frac{L_1}{L_3}, E_2 = -\frac{K_2}{K_3} \quad (25)$$

Figure 7 is a block diagram with this controller.

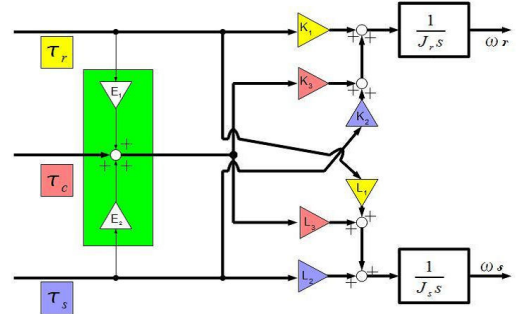


Fig. 7. Block diagram with FF controller

It is not so easy to derive these optimal ratios based on the physical value calculation, however, they can be identified by a PID controller. For this identification, a certain amount of the torque is applied only to the sun gear or ring gear respectively. Then the carrier torque is controlled to decouple the effect of sun/ring gear torque to the other side.

For example, in the case of  $E_1$  identification,  $\tau_r$  is set to 1 and  $\tau_s$  is set to 0. Based on Eq. (21),  $\tau_r$  will accelerate  $\theta_s$  as well as  $\theta_r$ . Then,  $\tau_c$  is decided by the PID control with the feedback of  $\theta_s$  in order to suppress the acceleration of  $\theta_s$ . The optimal ratio  $E_1$  is the ratio between the carrier torque  $\tau_c$  to the ring torque ( $\tau_r$ ) when the carrier torque suppresses the acceleration of  $\theta_s$ .  $E_2$  can be identified in the same way. Figure 8 is the illustration of this PID control.

This control algorithm is very simple feedforward control and the isolation ratio is subject to change by influence of friction and the posture of the robot arm. Therefore, we have to identify these isolation ratios periodically and need to have a table of the ratio with regard to the posture of the arm.

3) *Feedback design of carrier motor torque based on disturbance observer:* A planetary gear system can be driven in a feedback way to realize a bi-articular driving system. The proposed method uses disturbance observers. Figure 9 shows



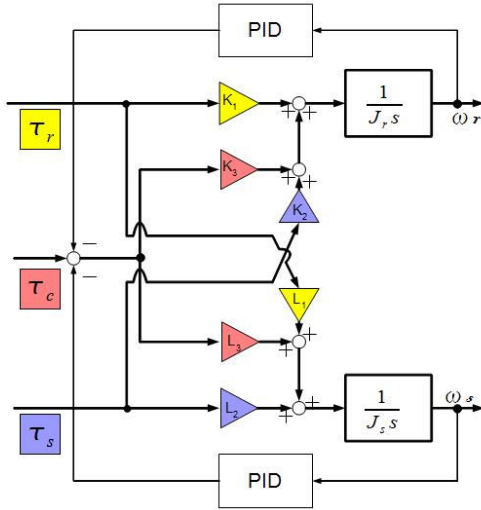


Fig. 8. Identifying by PID controller

a block diagram of a planetary gear system with disturbance observers.

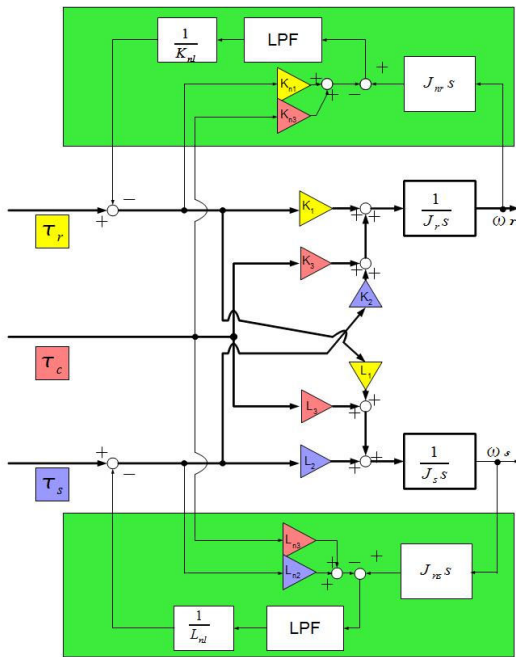


Fig. 9. Block diagram with disturbance observer

Disturbance observers observe influences from the other side mono-articular muscles as a disturbance and remove the disturbance by the feedback loop. Meanwhile, a disturbance observer can make a plant act as a nominal model. Due to this characteristic, if nominal models are set equal in both sides, the influence of the bi-articular muscle can be transmitted equally.

The point that should be noted is that the input to the nominal plant is the addition of  $\tau_s$  and  $\tau_c$  for the sun gear plant and  $\tau_r$  and  $\tau_c$  for the ring gear, which means the

nominal plant for each gear is designed based on Equation (8). With this nominal plant design, a planetary gear system described by Equation (20) and (21), are modified into the bi-articular driving system described in Equation (8). In next section, we will show that this control method is effective via simulation results.

## V. EXPERIMENTAL VERIFICATION OF BIARTICULAR MUSCLE COORDINATED FORCE CONTROL

In order to verify the suggested statics, experiments are conducted with a robot manipulator. We have developed a robot manipulator that incorporates the biarticular muscle mechanism [10]. Three motors are connected using a planetary gear system so as to realize two monoarticular muscles and one biarticular muscle. There are other types of biarticulated robot arm that also adopts a planetary gear system [9]. Our approach, however, focuses more on the development of control algorithm. The disturbance observer approach is adopted to make the planetary gear system work correctly as the biarticular muscle system. The configuration and detailed control algorithm are reported in our previous paper [10].

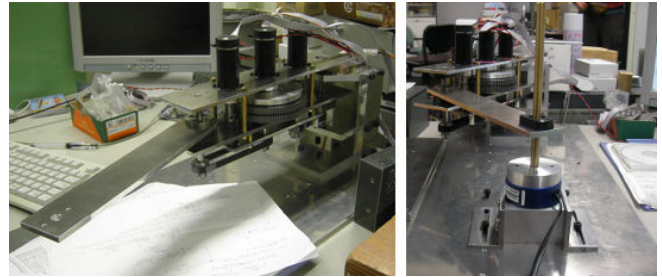
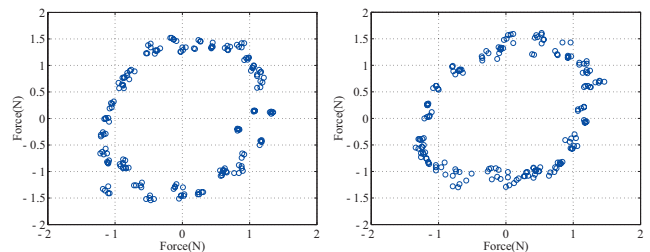


Fig. 10. Experimental Setup of Robot Manipulator with Biarticular Muscle

Figure 10 is the experimental setup (In this robot, the lengths of two links ( $l_1, l_2$  in Figure 3) are set same). A force sensor is attached to the end of the second link so that it can measure the force at the endeffector. In the experiments, the torques  $\tau_1^m$  and  $\tau_3^m$  in Equation (15) is applied changing the direction  $\theta_f$  under a constant value of  $F$ .

Two kinds of experiments are conducted: (a)  $\theta_2$  set to 120 degrees and (b)  $\theta_2$  set to 90 degrees. 180 points between 0 to 360 degrees are given as  $\theta_f$  increasing by 2 degrees. The following figure 11, 12 are the experimental result.



(a)  $\theta_2$  is set to 120 degrees (b)  $\theta_2$  is set to 90 degrees

Fig. 11. Experimental Verification of the Proposed Statics (Magnitude)

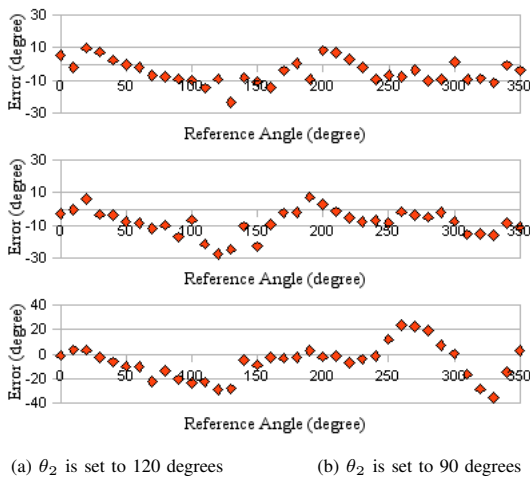


Fig. 12. Experimental Verification of the Proposed Statics (Direction)

Figure 11 shows the magnitudinal tracking performance. With the design  $F = 1.2$ , the force generated at the endeffector is supposed to draw a circle with a radius of 1.2N. Even though there is some distortion, the result shows a circular force trajectory. Figure 12 shows the directional tracking error that shows the error between the reference  $\theta_f$  and the measured angle. The result shows that, even though there are some magnitudinal errors due to the mechanical characteristics of torque-transmitting belts, the forces at the endeffector are generated in the designed directions.

## VI. CONCLUSIONS AND FUTURE WORKS

In this paper, a novel statics simplified by the biarticular muscle coordinate is suggested. Based on the simplified statics, force control at the endeffector is suggested. This force control algorithm is verified by experiments.

Experiments is conducted using a planetary gear driven robot arm. Planetary gear is used to emulate the musculoskeletal system that has two monoarticular muscle and one biarticular muscle. Feedback control algorithm is suggested to achieve this emulation. The result is successful showing that the suggested statics can be useful to be used as a novel simplified statics control.

The simple force control suggested in this paper is significant in terms of reaction force control. Since the suggested statics is simple that the reaction force at the endeffector by the angle feedback control of each joint can be easily designed [11], [12], [13]. Experiments of this reaction force control are future work.

Redundancy problem [14] is another issue. Even though only two actuators are used among three actuators consisting of two monoarticular muscle and one biarticular muscle in order to simplify the statics in this paper, redundancy of these three actuators can be utilized to make the actuator output more efficient.

## REFERENCES

- [1] D. W. Franklin, G. Liaw, T. E. Milner, R. Osu, E. Burdet, M. Kawato, "Endpoint Stiffness of the Arm Is Directionally Tuned to Instability in the Environment", *Journal of Neuroscience*, vol. 27(29), 2007, pp. 7705-7716
- [2] S. Stroeve, "Impedance Characteristics of a Neuromusculoskeletal Model of the Human Arm I. Posture Control", *Biological Cybernetics*, vol. 81, 1999, pp.475-494.
- [3] H. Gomi, M. Kawato, "Task-Dependent Viscoelasticity of Human Multijoint Arm and Its Spatial Characteristics for Interaction with Environments", *Journal of Neuroscience*, vol. 18(21), 1998, pp. 8965-8978.
- [4] N. Hogan, "Impedance Control: An Approach to manipulation: Part II - Implementation", *Journal of Dynamic Systems, Measurement, and Control*, vol. 107, 1985, pp. 8-16.
- [5] M. Kumamoto, T. Oshima, T. Yamamoto, "Control Properties Induced by the Existence of Antagonistic Pairs of Bi-articular Muscles - Mechanical Engineering Model Analyses", *Human Movement Science*, vol. 13, 1994, pp. 611-634.
- [6] R. Jacobs, MF. Bobbert, GJ. van Ingen Schenau, "Mechanical Output from Individual Muscles during Explosive Leg Extensions: The Role of Biarticular Muscles", *Journal of Biomechanics*, vol.29, no.4, 1996, pp.513-523.
- [7] G. J. van Ingen Schenau, M. F. Bobbert, and R. H. Rozend, "The Unique Action of Bi-articular Muscles in Complex Movements", *Journal of Anatomy*, vol.115, 1987, pp.1-5.82.
- [8] S. Oh, Y. Hori, "Development of Novel Two-Degree-of-Freedom Control for Robot Manipulator with Biarticular Muscle Torque", *American Control Control*, 2009, pp.325-330.
- [9] A. Umemura, Y. Saito, T. Haneyoshi, "The Rigidity of the Bi-articular Robotic Arm with a Planetary Gear", *Proc. of the IEEE Workshop on Advanced Motion Control*, 2010, pp.490-495.
- [10] Y. Kimura, S. Oh, Y. Hori, "Novel Robot Arm with Bi-articular Driving System Using a Planetary Gear System", *Proc. of the IEEE Workshop on Advanced Motion Control*, 2010, pp.296-301.
- [11] T. Takuma, S. Hayashi, K. Hosoda, "3D Bipedal Robot with Tunable Leg Compliance Mechanism for Multi-modal Locomotion", *Proc. of the IEEE/RSJ IROS 2008*, 2008, pp.1097-1102.
- [12] R. Niyama, A. Nagakubo, Y. Kuniyoshi, "Mowgli: A Bipedal Jumping and Landing Robot with an Artificial Musculoskeletal System", *Proc. of the 2007 IEEE ICRA*, 2007, pp.2546-2551.
- [13] S. Oh, Y. Kimura, Y. Hori, "Reaction Force Control of Robot Manipulator Based on Biarticular Muscle Viscoelasticity Control", *Proc. of the IEEE/ASME Advanced Intelligent Mechatronics*, 2010, pp.1105-1110.
- [14] B. Siciliano, "Kinematic Control of Redundant Robot Manipulators: A Tutorial", *Journal of Intelligent and Robotic Systems*, 1990, pp.201-212.